PERGAMON

International Journal of Heat and Mass Transfer 44 (2001) 1857–1867

International Journal of HEAT and MASS TRANSFER

www.elsevier.com/locate/ijhmt

A computer-aided parametric analysis of mixed convection in ducts

G.J. Hwang [a], S.C. Tzeng [a], C.Y. Soong [b,*]

[a] *Department of Power Mechanical Engineering, National Tsing Hua University, Hsinchu, Taiwan 30043, ROC*
[b] *Rotating Fluids and Vortex Dynamics Laboratory, Department of Aeronautical Engineering, Chung Cheng Institute of Technology, Taoyuan, Taiwan 33509, ROC*

Received 29 October 1999; received in revised form 12 July 2000

Abstract

This study develops a novel technique of computer-aided parametric analysis (CAPA) to formulate simple correlations for thermal flow characteristics in a complex convective flow system. To demonstrate the validity of the technique, fully developed mixed convection in uniformly heated horizontal ducts of square and circular cross-sections are employed as illustrative examples. The effects of secondary flow generated by the thermal buoyancy force are included. The CAPA technique employs characteristic quantities, constant factors and multi-term relationships to convert the governing equations into a set of algebraic equations. Relatively, this technique generates more extensive results than the conventional order-of-magnitude and scaling analyses. With the aid of limited data from numerical results (or measurements), formulas for evaluating the cross-sectional averages of axial velocity and temperature, the strength of secondary vortices, friction factors and the heat transfer rates at various *Pr* and *ReRa* can be derived. Comparisons of the present results and the direct numerical solutions manifest quite satisfactory performance of the CAPA technique. Merits of the CAPA technique are: (1) less effort required in the developing procedure, (2) clear parameter-dependence of the thermal flow characteristics, and (3) convenience in using the resultant correlations of algebraic form.

Keywords: Computer-aided parametric analysis; Mixed convection; Duct flow; Secondary flow effect; Friction and heat transfer correlations

1. Introduction

In the 17th century, Newton originated the concept of dynamical similarity. Forty years later, Euler was the first who discussed unit and dimensions in physical relationships. In 1822, Fourier applied the geometrical concept of dimension to physical quantities in heat flow problems. Near the end of the 19th century, Reynolds, Rayleigh, and many other researchers [1] successfully applied the idea of dimensional analysis. Vaschy in 1892, Riabouchinsky in 1911 and Buckingham [2,3] reported the establishment of the PI method. Buckingham outlined the general procedure of dimensional analysis. Although the number of non-dimensional parameters depends on the number of governing dimensional variables and their rank of dimensional matrix, there are many combinations of the dimensionless parameters. Consequently, little progress has been made after the early stage of development.

In recent years, great progress has been made in numerical simulation of physics and engineering, but the direct numerical computation of full Navier–Stokes equations and the energy equation is still not cost-effective. In addition, even with a large amount of numerical results, it is still not very easy to extract the parametric dependence and the physical senses involved. Therefore, simplification of the equations through physical consideration is indispensable. Schlichting [4] successfully applied an order-of-magnitude analysis

* Corresponding author. Tel.: +886-3-390-8102; fax: +886-3-389-1519.
E-mail address: cysoong@ccit.edu.tw
http://www.ccit.edu.tw/~RFVDLab (C.Y. Soong).

0017-9310/01/$ - see front matter
PII: S0017-9310(00)00245-3

Nomenclature

A	cross-sectional area (m^2)
A_i, A_i', A_i''	constant factors, $i = 1, 2, \ldots, 6$
C	parameter $= -C_1 D_e^3/4\mu v = Re/\overline{w}$
C_1	axial pressure gradient $= dP_o/dZ$ (N/m^3)
C_2	axial temperature gradient $= \partial T/\partial Z$ (K/m)
D_e	equivalent hydraulic diameter $= 4A/S$ (m)
f	friction factor $= 2\overline{\tau}_w/\rho\overline{W}^2$
g	gravitational acceleration (m/s^2)
$\overline{h}$	average heat transfer coefficient ($W/(m^2\,K)$)
K_f	thermal conductivity of fluid (W/(m K))
Nu	Nusselt number $= \overline{h}D_e/K_f$
P_o	axial pressure distribution which is a function of Z only (N/m^2)
Pr	Prandtl number $= v/\alpha$
q	constant wall heat flux (W/m^2 s)
Ra	Rayleigh number $= g\beta C_2 D_e^4/v\alpha$
Re	Reynolds number $= \overline{W}D_e/v$
S	circumference of cross-section (m)
T	local temperature (K)
T_w	wall temperature (K)
U, V, W	velocity components in X, Y and Z directions or in R, ϕ and Z directions (m/s)
u, v, w	dimensionless velocity components in x, y and z directions or in r, ϕ and z directions
X, Y, Z	Cartesian coordinates (m)
x, y, z	dimensionless Cartesian coordinates

Greek symbols

α	thermal diffusivity (m^2/s)
β	coefficient of thermal expansion (1/K)
θ	dimensionless temperature difference $= (T - T_w)/(C_2 D_e PrC)$
μ	viscosity ($N\,s/m^2$)
v	kinematic viscosity (m^2/s)
Ξ, ξ	dimensional and dimensionless vorticity (unit of Ξ is 1/s)
ρ	density (kg/m^3)
τ_w	wall shear stress (N/m^2)
Ψ, ψ	dimensional and dimensionless stream function (unit of Ψ is m^2/s)

Superscript

$\overline{(\ )}$	cross-sectionally averaged quantity

Subscripts

b	bulk quantity
c	characteristic quantity
o	condition for pure forced convection
q	constant wall heat flux
w	wall condition

(OMA) to the boundary layer flow over a flat plate. Cheng et al. [5] used the same technique to analyze mixed convection flow in the thermal entrance region of horizontal rectangular channels. One can derive dimensionless parameters from the ratios of individual terms in the governing equations and the associate boundary conditions. However, the OMA technique derives no simple algebraic relations among these parameters.

The technique of using a two-term relation from the physical similitude is known as scaling or scale analysis (SA). Bejan [6] applied this SA technique to various heat transfer problems. Krane and Incropera [7] reported a scaling analysis of the unidirectional solidification of a binary alloy. Due to the flow complexity, the two-term relationship from the physical similitude may not fully describe the mechanism of transport phenomena. The conventional scaling analysis deals with a simple flow system by comparing two terms in balance equations to get the order-of-magnitude of certain physical quantity. For a complex flow problem, only some dimensionless parameters can be resulted by this class of techniques. Multiple-term relation would be more appropriate. In a recent work by Soong and Chyuan [8], for example, three and four terms of tangential and radial momentum equations, respectively, were used to develop concise and rational correlation for buoyancy effects in rotation-induced mixed convection flow.

The purpose of this study is to develop a technique of parametric analysis of mixed convection. By formulating and solving a set of simple algebraic equations and invoking the aid of less numerical solutions or experimental data, a functional relationship between thermal-flow characteristics and the governing parameters can be formulated. In the cases considered in the present work, only two point data obtained by numerical computations (or experimental data) are needed to determine the constant factors in the correlation. To keep the complete physical effects, in the present computer-aided parametric analysis (CAPA) technique, all terms in the momentum and energy balance equations are retained. Simple expressions of the secondary flow effects are also introduced into the correlation. Finally, a set of correlations for flow and heat transfer characteristics of mixed convection with the presence of secondary flow can be completed.

2. Basic equations

The thermal fluid flow considered in the present study is steady and laminar in a hydrodynamically and

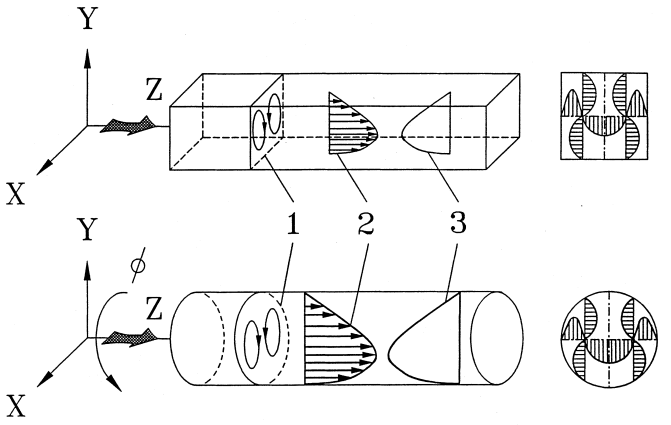

Fig. 1. Physical models and coordinate system.

thermally fully developed region of a horizontal square duct or a horizontal circular pipe. The axial pressure and temperature gradients are constant and the peripheral wall temperature is uniform. Fig. 1(a) displays the physical model and the coordinate system. In the present analysis, Cartesian coordinates system is applied to both cases of square channel and circular pipe. The viscous dissipation and compressibility effects in the energy equation are neglected. The Boussinesq approximation is assumed to be valid. After a cross-differentiation in cross-sectional plane, the governing equations for a thermal flow fully developed in Z direction [9] are written as

$$U(\partial\Xi/\partial X)+V(\partial\Xi/\partial Y)=\nu\nabla^2\Xi+\beta g(\partial T/\partial X), \tag{1}$$

$$U(\partial W/\partial X)+V(\partial W/\partial Y)=-1/\rho(\partial P_o/\partial Z)+\nu\nabla^2 W, \tag{2}$$

$$U(\partial T/\partial X)+V(\partial T/\partial Y)+W(\partial T/\partial Z)=\alpha\nabla^2 T, \tag{3}$$

where

$$\Xi=-\nabla^2\Psi=\partial V/\partial X-\partial U/\partial Y, \tag{4a}$$

$$U=\partial\Psi/\partial Y,\qquad V=-\partial\Psi/\partial X. \tag{4b}$$

By employing the following dimensionless variables and parameters,

$$\begin{aligned}&x=X/D_e,\quad y=Y/D_e,\quad u=UD_e/\nu,\\&v=VD_e/\nu,\quad w=WD_e/(\nu C),\\&\theta=(T-T_w)/C_2D_ePrC,\quad C_1=\partial P_o/\partial Z,\\&C_2=\partial T/\partial Z,\quad C=-(C_1D_e^3)/4\nu\mu,\\&Ra=g\beta C_2D_e^4/\nu\alpha,\quad Pr=\nu/\alpha,\end{aligned} \tag{5}$$

Eqs. (1)–(3) can be cast into the dimensionless form,

$$u(\partial\xi/\partial x)+v(\partial\xi/\partial y)=\nabla^2\xi+RaC(\partial\theta/\partial x), \tag{6}$$

$$u(\partial w/\partial x)+v(\partial w/\partial y)=\nabla^2 w+4, \tag{7}$$

$$Pr[u(\partial\theta/\partial x)+v(\partial\theta/\partial y)]=\nabla^2\theta-w, \tag{8}$$

and the vorticity and stream function relations, (4a) and (4b), become

$$\xi=-\nabla^2\psi=\partial v/\partial x-\partial u/\partial y, \tag{9a}$$

$$u=\partial\psi/\partial y,\qquad v=-\partial\psi/\partial x, \tag{9b}$$

where $\nabla^2=(\partial^2/\partial x^2+\partial^2/\partial y^2)$. The solution contains two independent parameters RaC and Pr [9]. The value of Pr ranges from 0 to 500 in the present study. Consequently, the boundary conditions at channel walls can be written as

$$\partial\psi/\partial n=w=\theta=0, \tag{10}$$

where n is a unit normal to the channel wall. The boundary value of stream function at the channel walls is $\Psi=0$. The symmetry condition is not assumed and the computation is performed over the whole cross-section of the channel and it demonstrates that the flow and temperature fields remain symmetric in the ranges of RaC and Pr considered. In the present work, the numerical solution of vorticity–velocity formulation, Eqs. (6)–(8), (9a) and (9b), plays a complementary role to support the development of CAPA. The PDE system is discretized by utilizing the power-law scheme [10]. The boundary–vorticity method [11] is used to solve the vorticity transport equation and the SIS algorithm [12] is

applied for solution of the resultant difference equations. The iteration is terminated when the variables satisfy the criterion as

$$\varepsilon = \sum_{i,j} \left| (F_{i,j}^{n+1} - F_{i,j}^{n})/F_{i,j}^{n+1} \right| \leqslant 5 \times 10^{-5},$$

where F represents Ψ, ξ, w, and θ. The subscripts i and j show the ith and the jth grid in x and y directions, respectively. The superscript n indicates the nth iteration. The numerical errors are less than 0.12%, when using the mesh points of 41×41. The detailed procedure of numerical solution has been given in the literature [9] and will not be repeated here.

After computation, C converts to the Reynolds number $Re = \overline{W} D_e/\nu$ by the relation $C = Re/\overline{w}$. Following the conventional definitions, the expressions for the friction parameter $f \cdot Re$ and the Nusselt number Nu are

$$f \cdot Re = (2\overline{\tau}_w/\rho \overline{W}^2)(\overline{W} D_e/\nu) = 2/\overline{w}, \tag{11}$$

$$Nu = h\overline{D_e}/K_f = \overline{w}/(4\overline{w\theta}/\overline{w}), \tag{12}$$

where $\overline{w}$ and $\overline{w\theta}$ are the cross-sectional averages evaluated by using Simpson's rule.

3. CAPA technique

3.1. Comparison of CAPA and other methods

Before developing the CAPA for the mixed convection flows in ducts, a comparison of CAPA and other techniques is to be presented first. In the CAPA analysis, the parametric correlations are directly derived from the governing equations and it is assumed that the profiles of velocity components and temperature distribution remain unchanged in their shapes but changed in magnitudes with governing parameters. Similar to the techniques of SA and OMA, the characteristic quantities are used for representing the corresponding flow variables, and the ratios of characteristic quantities for the derivatives in the governing equation. As shown in Table 1, the CAPA technique introduces a positive or negative sign by considering the physical meaning of each term in the governing equation. On the contrary, the SA and OMA techniques do not consider any sign. The CAPA technique also uses constant factors to make up the difference in the magnitudes of the ratios of characteristic quantities and the derivatives. Finally, the PI method shows only an unknown function with non-dimensional parameters, the SA technique yields only dimensionless parameters, and the OMA technique provides the dimensionless partial differential equations with non-dimensional parameters. The present CAPA technique will give a set of algebraic equations with parameters. As seen in Table 1, the OMA and CAPA techniques can fully describe the physics in the transport phenomena of the problem. The present CAPA technique dramatically simplifies the process in solving a set of algebraic equations instead of solving PDE with the OMA technique.

3.2. Development of parametric analysis by CAPA technique

Consider the case of $Pr = 0.73$ and $RaC = 10^5$ ($ReRa = 1.385 \times 10^4$), Fig. 2(a) shows the dimensionless isotherms and constant axial velocity lines and Fig. 2(b) shows the stream function and secondary flow velocity vector on cross-plane of a square duct. To illustrate the CAPA technique, Fig. 2(c) shows the schematic diagram for dimensional temperature and axial velocity on the plane $x = 0.5$. Fig. 2(d) depicts the secondary flow velocities on the planes $x = 0.25$, $x = 0.75$ and $y = 0.5$. The present CAPA technique assumes that

Table 1
Comparison of PI method, SA, OMA and CAPA techniques

Characterstics	Analysis			
	PI method	SA[a]	OMA	CAPA
Sign	NA	+	PDE	±
Factor	NA	Unit	PDE	Constant
T–T relation[b]	NA	One–one	One–one	Multiple terms
Equation for N-D. parameters[c]	Unknown function	NA[d]	PDE[e]	Algebraic
Physics in T.P.[f]	No	May be partially	Fully	Fully

[a] SA: Scale analysis based on the book written by Bejan [6].
[b] T–T: Term to term.
[c] N-D: Non-dimensional.
[d] NA: Not applicable.
[e] PDE: Partial differential equation.
[f] T.P.: Transport phenomena.

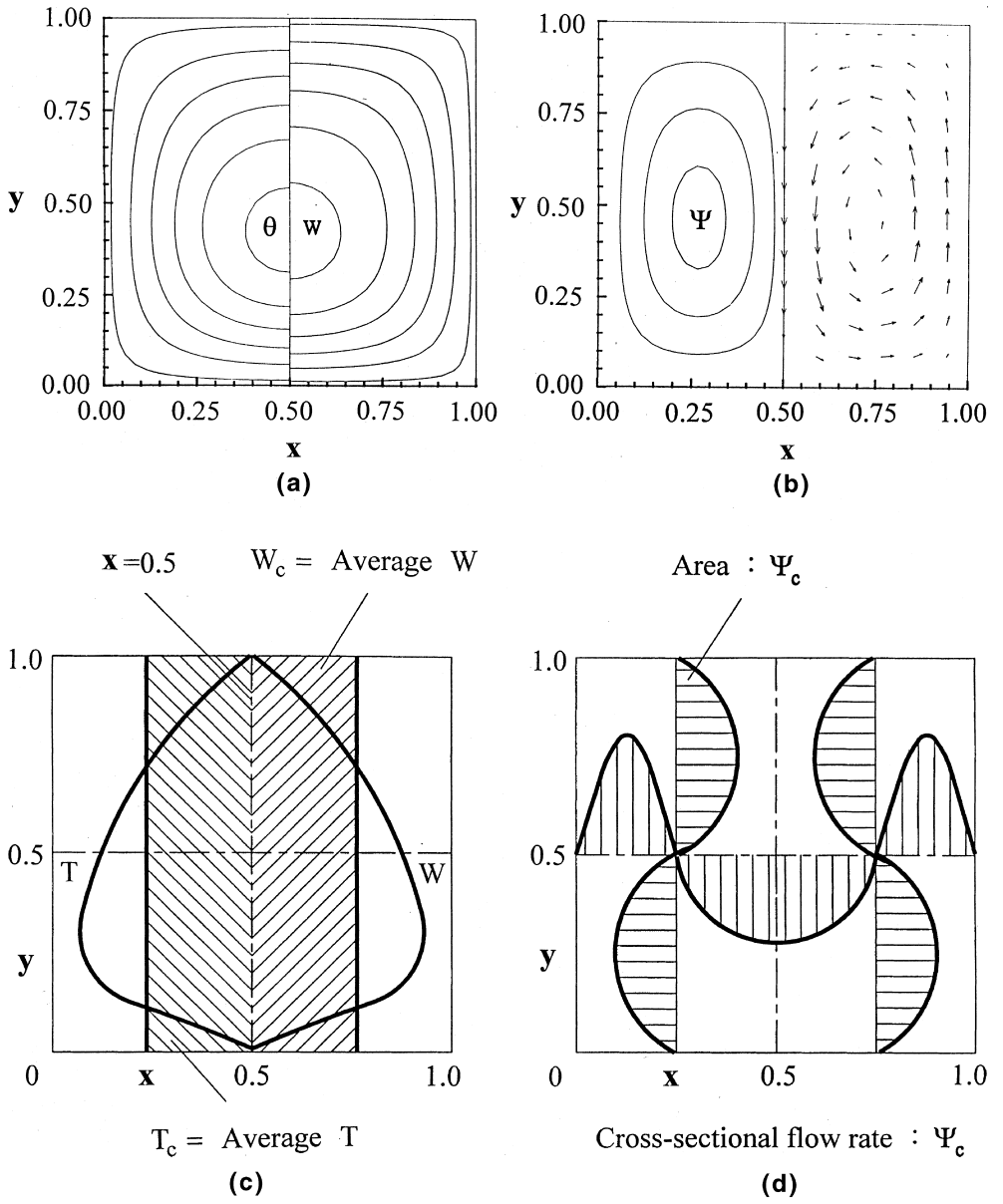

Fig. 2. Field and cross-sectional average properties of mixed convection at $Pr = 0.73$ and $RaC = 10^5$ in a square duct: (a) temperature and axial velocity; (b) stream function and vector distributions; (c) averages or characteristic quantities of temperature and axial velocity; (d) cross-sectional flow rate.

the temperature, axial velocity, and secondary flow patterns in the ranges of parameters investigated do not deviate much from the ones shown in this figure. The cross-sectional averages of temperature and the axial velocity, respectively, are considered as the characteristic temperature and axial velocity, and the maximum value of the stream function on the cross-plane is used to characterize the total secondary flow rate.

In working procedure of the CAPA technique, by employing the properly defined characteristic quantities for dependent and independent variables, the original PDEs are then turned into that of algebraic form. Each term involves a constant factor in order to make up the approximations. In a resultant equation of n terms, actually, only $(n-1)$ terms need this kind of factors. For example, with scales of the velocity components and their derivatives

$$U = \partial\Psi/\partial Y \approx \Psi_c/D_e, \quad V = -\partial\Psi/\partial X \approx -\Psi_c/D_e,$$
$$\partial W/\partial X \approx W_c/D_e,$$

$$\partial W/\partial Y \approx W_c/D_e, \quad \partial W/\partial X^2 \approx -W_c/D_e^2,$$
$$\partial^2 W/\partial Y^2 \approx -W_c/D_e^2,$$

and the factors A_4' and A_4'', the terms in the axial momentum Eq. (2) can be expressed as

$$U(\partial W/\partial X) + V(\partial W/\partial Y) \approx A_4'(\Psi_c/D_e)(W_c/D_e), \quad (13a)$$
$$-1/\rho(\partial P_o/\partial Z) = -C_1/\rho, \quad (13b)$$
$$\nu\nabla^2 W \approx -A_4''\nu W_c/D_e^2. \quad (13c)$$

Combining Eqs. (13a)–(13c) with $A_4 \equiv A_4'/A_4''$ and $A_3' \equiv 1/A_4''$, finally, one has an algebraic relation

$$A_4\frac{\Psi_c}{D_e}\frac{W_c}{D_e} = -\frac{C_1}{\rho}A_3' - \nu\frac{W_c}{D_e^2} \quad (14a)$$

or

$$W_c = A_3'\left(-\frac{C_1}{\rho}\right)\Big/\left(A_4\frac{\Psi_c}{D_e^2} + \frac{\nu}{D_e^2}\right). \quad (14b)$$

It is seen that the inertia term of the original equation is replaced by $A_4(\Psi_c/D_e)(W_c/D_e)$, in which the ratio Ψ_c/D_e stands for the mean secondary flow velocity U, Ψ_c indicates the maximum value of stream function at vortex center, W_c represents the mean axial velocity, and the constant A_4 makes up the difference between the magnitudes of $U(\partial W/\partial X) + V(\partial W/\partial Y)$ and $(\Psi_c/D_e)(W_c/D_e)$. The first term with a constant A_3' on the RHS of Eq. (14a) represents the pressure-gradient term. The last one with a negative sign is for the viscous term. Eqs. (14a) and (14b) tells that the pressure gradient drives the flow and is balanced by the inertia force and the viscous force. This describes the physics of transport phenomena.

Following the procedure mentioned above, the energy equation (3) is turned into

$$A_6\frac{\Psi_c}{D_e}\frac{T_c - T_w}{D_e} + A_5 W_c C_2 = -\alpha\frac{T_c - T_w}{D_e^2} \quad (15a)$$

or

$$T_c - T_w = -A_5 W_c C_2\Big/\left(A_6\frac{\Psi_c}{D_e^2} + \frac{\alpha}{D_e^2}\right) \quad (15b)$$

where $(T_c - T_w)$ indicates the mean temperature difference between the fluid and the wall. Thermal convection in the axial direction, $-A_5 C_2 W_c$, is balanced by the thermal convection, $A_6(\Psi_c/D_e)(T_c - T_w)/D_e$, and the heat conduction, $\alpha(T_c - T_w)/D_e^2$.

For the vorticity transport equation (1), one has

$$A_1\frac{\Psi_c}{D_e}\frac{1}{D_e}\frac{\Psi_c}{D_e^2} = -\nu\frac{\Psi_c}{D_e^4} - A_2'\beta g\frac{T_c - T_w}{D_e} \quad (16a)$$

or

$$A_1\Psi^2 + \Psi - A_2'\beta g(T_c - T_w)\frac{D_e^3}{\nu^2} = 0. \quad (16b)$$

In Eq. (16a), $\Xi_c = \Psi_c/D_e^2$ is used to approximate $\Xi = -\nabla^2\Psi$ in Eq. (1). By substituting $(T_c - T_w)$ in Eq. (15b) into (16b) and introducing dimensionless stream function $\psi = \Psi_c/\nu$ and $A_2 \equiv A_2'A_5$, one has

$$A_1\psi^2 + \psi + \frac{A_2'A_5}{A_6 Pr\psi + 1}ReRa = 0 \quad (17a)$$

or

$$\psi^3 + \frac{A_1 + A_6 Pr}{A_1 A_6 Pr}\psi^2 + \frac{1}{A_1 A_6 Pr}\psi - \frac{A_2}{A_1 A_6 Pr}ReRa = 0. \quad (17b)$$

From [13], the solution of the above cubic equation is

$$\psi = M + N - \frac{\alpha_1}{3} \quad (\text{as } Q > 0),$$
$$= 2\sqrt{-Q}\cos\left(\frac{\phi}{3}\right) - \frac{\alpha_1}{3} \quad (\text{as } Q < 0), \quad (18)$$

where

$$\alpha_1 = \frac{A_1 + A_6 Pr}{A_1 A_6 Pr}, \quad \alpha_2 = \frac{1}{A_1 A_6 Pr}, \quad \alpha_3 = -\frac{A_2}{A_1 A_6 Pr}ReRa,$$

$$Q = \frac{3\alpha_2 - \alpha_1^2}{9}, \quad R = \frac{9\alpha_1\alpha_2 - 27\alpha_3 - 2\alpha_1^2}{54},$$

$$M = \sqrt[3]{R + \sqrt{Q^3 + R^2}}, \quad N = \sqrt[3]{R - \sqrt{Q^3 + R^2}},$$
$$\cos\phi = \frac{R}{\sqrt{-Q^2}}.$$

By employing the dimensionless mean velocity $\overline{w} = W_c D_e/\nu C$ and temperature $\overline{\theta} = (T_c - T_w)/C_2 D_e Pr C$ and putting $A_3 = 4A_3'$, Eqs. (14b) and (15b) change to the dimensionless forms,

$$\overline{w} = \frac{A_3}{1 + A_4\psi}; \quad (19)$$

$$\overline{\theta} = \frac{-A_5\overline{w}}{1 + A_6 Pr\psi}. \quad (20)$$

Instead of solving ψ shown in Eq. (18), one may also solve it reversely by finding the value of $ReRa$ in Eq. (17a) and (17b) with an increment of ψ from the zero value, i.e.,

$$ReRa = [A_1\psi + (1 + A_1 A_6)\psi^2 + A_6 Pr\psi^3]/A_2. \quad (21)$$

With this value of ψ, one may obtain the dimensionless mean axial velocity $\overline{w}$ and mean temperature difference $\overline{\theta}$ from Eqs. (19) and (20) for the corresponding $ReRa$.

Following the conventional definitions of $f \cdot Re$ in Eq. (11), one can readily obtain the ratio of friction factors as

$$f \cdot Re/(f \cdot Re)_o = 1 + A_4\psi, \quad (22)$$

where $(f \cdot Re)_o = A_3$ by considering $\psi = 0$ at $ReRa = 0$. For the definition of Nu in Eq. (12), the mixed mean temperature difference $\overline{w\theta}/\overline{w}$ is the same as the mean temperature difference, $\overline{\theta}$ in the CAPA technique. Consequently, the Nusselt number relation is

$$Nu/(Nu)_o = 1 + A_6 Pr\psi, \tag{23}$$

where $(Nu)_o$ is the Nusselt number for $\psi = 0$. Eqs. (22) and (23) give simple expressions of the effects of secondary flow on the friction factor and Nusselt number, respectively. The present expressions (22) and (23) are disclosed in the literature for the first time.

3.3. Limiting case of $Pr \to 0$

For the case of $Pr \to 0$, the thermal convection in the flow direction is balanced by the conductive heat transfer in the cross-sectional plane. The convection term in the cross-sectional plane is not important. By using the characteristic quantities, the energy equation becomes

$$A_5 W_c C_2 = -\alpha \frac{T_c - T_w}{D_e^2} \tag{24a}$$

or

$$T_c - T_w = -A_5 W_c C_2 \Big/ \left(\frac{\alpha}{D_e^2}\right). \tag{24b}$$

By substituting $(T_c - T_w)$ into the vorticity transport equation (16b), one has

$$A_1\psi^2 + \psi - A_2 ReRa = 0. \tag{25}$$

This equation can be obtained readily by multiplying Eq. (17b) by $A_1 A_6 Pr$ and putting $Pr = 0$. The solution for positive ψ is

$$\psi = -\frac{1}{2A_1} + \sqrt{\frac{1}{4A_1^2} + \frac{A_2}{A_1} ReRa}. \tag{26}$$

The ratio of friction factors can be written as a function of $ReRa$.

$$\frac{f \cdot Re}{(f \cdot Re)_o} = 1 + A_4\psi = 1 + \frac{A_4}{2A_1}\left(\sqrt{1 + 4A_1A_2 ReRa} - 1\right). \tag{27}$$

Note that the Nusselt number ratio is $Nu/(Nu)_o = 1.0$ for $Pr = 0$.

3.4. Limiting case of $Pr \to \infty$

In the case of large Prandtl number, $Pr \to \infty$, the buoyancy force is balanced by the viscous force in the vorticity transport equation (16a), i.e.,

$$0 = \nu - \frac{\psi}{D_e^4} - A_2'\beta g \frac{T_c - T_w}{D_e}. \tag{28}$$

By substituting $(T_c - T_w)$ of Eq. (5) into (8), one has

$$\psi^2 + \frac{1}{A_6 Pr}\psi - \frac{A_2}{A_6 Pr} ReRa = 0. \tag{29}$$

Then one has a positive solution for ψ,

$$\psi = -\frac{1}{2A_6 Pr} + \sqrt{\frac{1}{4A_6^2 Pr^2} + \frac{A_2}{A_6 Pr} ReRa}. \tag{30}$$

The value of stream function will be zero for finite $ReRa$ and $Pr \to \infty$. The zero limiting value can be observed also from Eq. (17b). The ratio of friction factors in Eq. (22) yields

$$\frac{f \cdot Re}{(f \cdot Re)_o} = 1 + A_4\psi = 1 + \frac{A_4}{2A_6 Pr}\left(\sqrt{1 + 4A_2A_6 PrReRa} - 1\right) = 1.0 \tag{31}$$

for an infinite Prandtl number. The ratio of Nusselt number becomes

$$\frac{Nu}{(Nu)_o} = 1 + A_6 Pr\psi = \frac{1}{2} + \sqrt{\frac{1}{4} + A_2 A_6 PrReRa}. \tag{32}$$

The constant factors can be determined by using a few data from numerical solutions of the governing PDEs (or the measurements if available). For $\psi = 0$ at $ReRa = 0$, the numerical data of pure forced convection determine A_3 and A_5. For a given Pr and $ReRa$, the mixed convection data determine A_4 and A_6. However, in the present study, the values of $ReRa$ are chosen by considering the minimum percentage RMS error at 11 points over the range of $ReRa$. Tables 2 and 3 list the factors $A_i,\ i = 1, 2, \ldots, 6$ for $Pr = 0$–500.

4. Results and discussion

In the present study, the CAPA technique yields simple correlations for combined free and forced laminar convection in ducts for Prandtl number ranging from 0 to 500 and $ReRa = 0$ to around 1×10^5. It covers the liquid metal for small Pr, gases, water, and engine oils for large Pr. The CAPA technique provides a method to derive simple and accurate correlation formulas of a complex thermal fluid flow with the support of only few data from numerical calculations or experimental measurements.

To demonstrate the effectiveness of the CAPA technique, flow pattern of one pair of counter-rotating vortices in mixed convection duct flows is selected. The value of the stream function is zero on the square

Table 2
The corresponding factors for mixed convection in a horizontal square duct[a]

Factors	Prandtl No. (Pr)						
	0	0.01	0.1	0.73	7.2	100	500
A_1	1.632×10^{-2}	1.846×10^{-2}	2.165×10^{-2}	1.128×10^{-1}	1.759	40.977	–
A_2	5.560×10^{-5}	5.560×10^{-5}	5.563×10^{-5}	5.561×10^{-5}	5.570×10^{-5}	5.577×10^{-5}	5.573×10^{-5}
A_4	1.362×10^{-2}	3.431×10^{-2}	4.347×10^{-2}	4.761×10^{-2}	2.434×10^{-2}	2.541×10^{-2}	2.581×10^{-2}
A_6	–	8.776×10^{-1}	1.080×10^{-1}	9.529×10^{-2}	8.906×10^{-2}	8.645×10^{-2}	7.992×10^{-2}

[a] $A_3 = 1.404 \times 10^{-1}$ and $A_5 = 4.820 \times 10^{-2}$ for all Prandtl numbers. These factors are evaluated at $ReRa = 14.0$ and 10,444.3 for $Pr = 0$, $ReRa = 14.0$ and 33,094.6 for $Pr = 0.01$, $ReRa = 14.0$ and 61,807.5 for $Pr = 0.1$, $ReRa = 14.0$, and 91,591.5 for $Pr = 0.73$, $ReRa = 14.0$, and 68,603.4 for $Pr = 7.2$, $ReRa = 14.0$, and 10,532.6 for $Pr = 100$, and $ReRa = 1.4$ and 140.2 for $Pr = 500$.

Table 3
The corresponding factors for mixed convection in a horizontal circular duct[a]

Factors	Prandtl No. (Pr)						
	0	0.01	0.1	0.73	7.2	100	500
A_1	6.909×10^{-2}	6.951×10^{-2}	7.482×10^{-2}	1.685×10^{-1}	2.172	3.408	–
A_2	7.743×10^{-4}	7.736×10^{-4}	7.736×10^{-4}	7.782×10^{-4}	7.791×10^{-4}	7.750×10^{-4}	7.750×10^{-4}
A_4	5.138×10^{-2}	6.174×10^{-2}	6.509×10^{-2}	4.188×10^{-2}	1.262×10^{-2}	1.044×10^{-2}	1.038×10^{-2}
A_6	–	1.870	3.124×10^{-1}	8.940×10^{-2}	5.248×10^{-2}	4.177×10^{-2}	3.577×10^{-2}

[a] $A_3 = 4.921 \times 10^{-1}$ and $A_5 = 1.903 \times 10^{-1}$ for all Prandtl numbers. These factors are evaluated at $ReRa = 49.2$ and 4054.5 for $Pr = 0$, $ReRa = 49.2$ and 4153.9 for $Pr = 0.01$, $ReRa = 49.2$ and 4166.7 for $Pr = 0.1$, $ReRa = 49.2$, and 92,182.8 for $Pr = 0.73$, $ReRa = 49.2$, and 4804.3 for $Pr = 7.2$, $ReRa = 49.2$, and 349.7 for $Pr = 100$, and $ReRa = 49.3$ and 147.8 for $Pr = 500$.

channel wall and along the centerline of symmetry, and it is maximum in the sense of absolute value at the center of counter-rotating vortices. The maximum value of the stream function may be regarded as the secondary flow rate of one of the vortices. It is seen that the stream function is a significant variable in the present parametric analysis. The relationships of the stream function and $ReRa$ to the Prandtl number in the range $Pr = 0$–500 are plotted in Fig. 3. The results show that the stream function of CAPA fits well with the numerical solutions. The RMS of the percentage error is about 2.79% for $Pr = 0.73$. The errors for the other Prandtl number are also shown in Fig. 3.

To illustrate the accuracy of the technique on the mean axial velocity, the numerical solution is used to obtain A_3 and A_4 in Eq. (19). In Fig. 4, comparison of the mean axial velocity with the numerical solution is made for various Prandtl numbers. A maximum of 0.58% difference from the numerical solution for $Pr = 0.73$ is observed. The differences for the other Prandtl numbers are also shown in Fig. 4.

The temperatures with $ReRa$ for $Pr = 0$–500 are shown in Fig. 5. The results of the simple algebraic equation of the CAPA technique agree well with numerical predictions. With the CAPA technique, the ratios of friction factor and Nusselt number can be expressed by Eqs. (22) and (23), respectively. Fig. 6 shows the friction parameter $f \cdot Re/(f \cdot Re)_o$ for $Pr = 0$–500

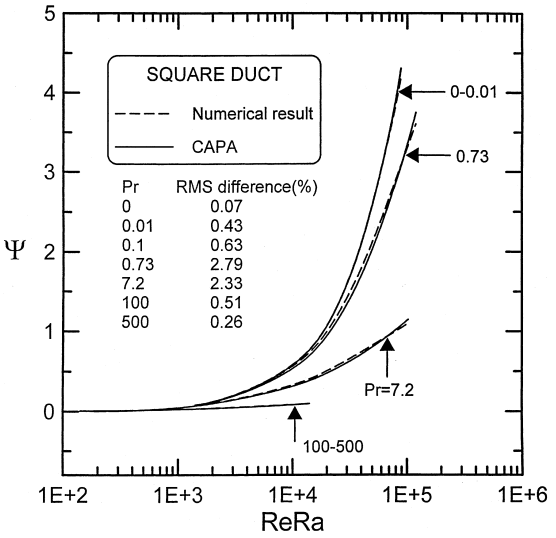

Fig. 3. Comparison between ψ predicted by CAPA and numerical solutions for mixed convection in a square duct.

with RMS difference in percentage. The maximum difference between the CAPA results and the numerical predictions is 0.65% for $Pr = 0.73$. Fig. 7 shows the comparisons of the evaluated buoyancy effects on heat transfer performance. It is noted that, as $Nu/(Nu)_o$ is

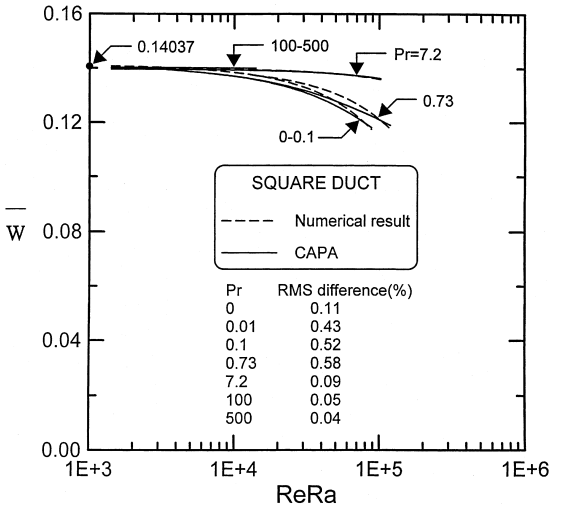

Fig. 4. Comparison between $\overline{w}$ predicted by CAPA and numerical solutions for mixed convection in a square duct.

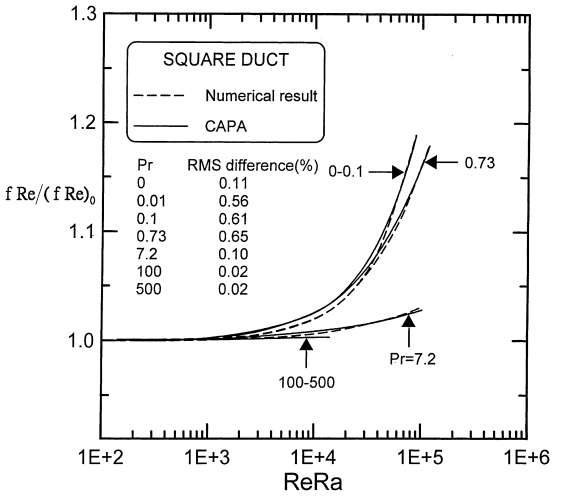

Fig. 6. Comparison between $f \cdot Re/(f \cdot Re)_o$ predicted by CAPA and numerical solutions for mixed convection in a square duct.

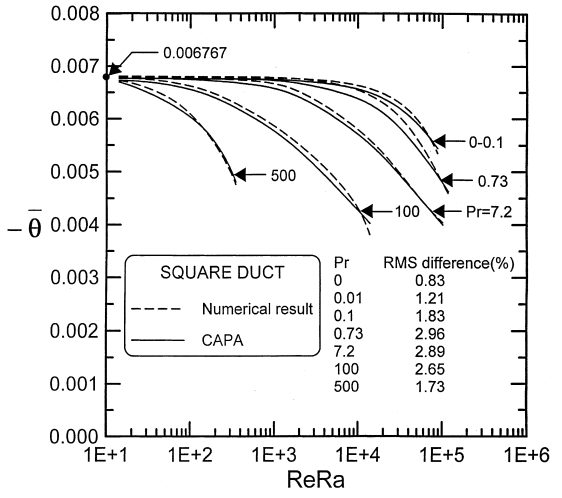

Fig. 5. Comparison between $\overline{\theta}$ predicted by CAPA and numerical solutions for mixed convection in a square duct.

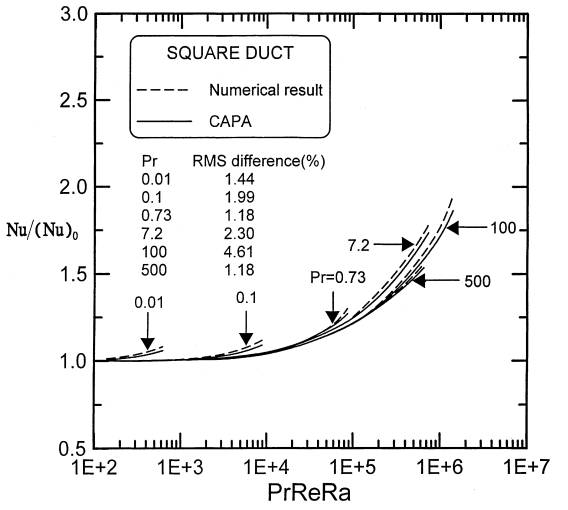

Fig. 7. Comparison between $Nu/(Nu)_o$ predicted by CAPA and numerical solutions for mixed convection in a square duct.

plotted vs *PrReRa* rather than *ReRa*, the curves at different *Pr* get close to each other and show weak *Pr*-dependence. The RMS differences of $Nu/(Nu)_o$ are slightly larger than those of $f \cdot Re/(f \cdot Re)_o$. This is due to an over-simplification of the non-linear term $\overline{w\theta}/\overline{w}$ to $\overline{\theta}$.

The corresponding results for circular ducts are shown in Figs. 8 and 9, respectively. These two figures demonstrate that the correlations (22) and (23) are also available to the mixed convection in circular ducts. For clarity, the value of *ReRa* is used in Fig. (9).

5. Conclusions

A technique of CAPA has been developed for deriving simple and quite accurate formulas with the aid of only few numerical data for a complex convective flow system. The CAPA technique formulates a set of algebraic equations from the original conservative equations with considerations of multi-term relationships, physical meaning, sign and scale of each term, and proper constant factors for approximation. It is much easier to solve the resultant algebraic equations of the

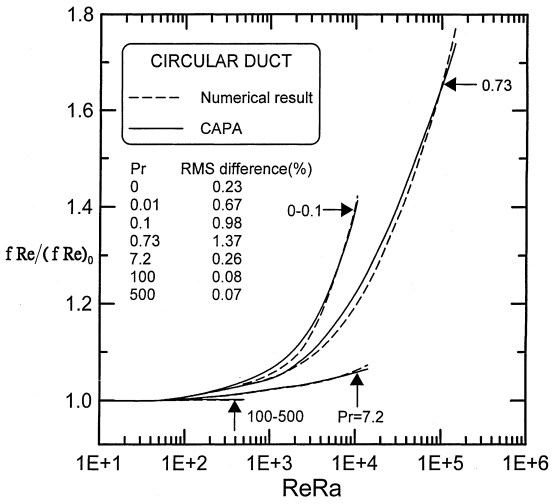

Fig. 8. Comparison between $f \cdot Re/(f \cdot Re)_o$ predicted by CAPA and numerical solutions for mixed convection in a circular duct.

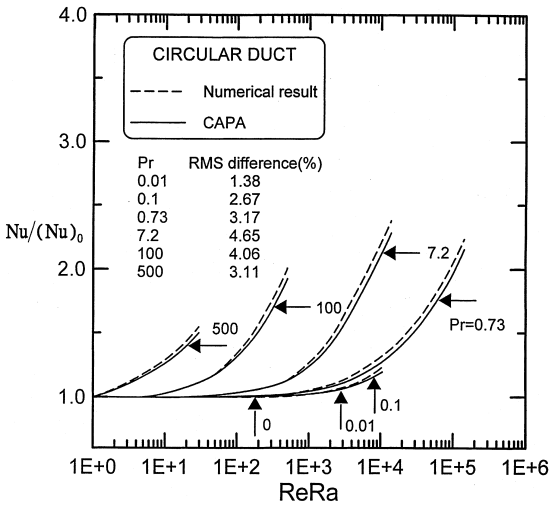

Fig. 9. Comparison between $Nu/(Nu)_o$ predicted by CAPA and numerical solutions for mixed convection in a circular duct.

characteristic quantities than to solve the original system of partial differential equations.

In the present study, the CAPA technique has been implemented to yield simple correlations for the laminar fully developed mixed convection in horizontal square and circular ducts for Prandtl numbers from 0 to 500 and $ReRa = 0$–1×10^5. The range of Prandtl numbers includes the liquid metal of small Pr, gases, water, and engine oils of large Pr. By the CAPA technique, the ratio of cross-sectional (peripheral) averages of friction factor, $f \cdot Re/(f \cdot Re)_o = 1 + A_4\psi$, and the ratio of Nusselt number, $Nu/(Nu)_o = 1 + A_6 Pr\psi$, are obtained. These two simple correlation equations have not been reported in the literature yet. The maximum deviation between the correlations and the numerical data is no more than a few percent for $Pr = 0$ to 500 and $ReRa = 0$–1×10^5.

For limiting cases of $Pr \to 0$ and $Pr \to \infty$, the ratios of friction factor and Nusselt number can be written explicitly in terms of $ReRa$ or $PrReRa$ in Eqs. (27), (31) and (32). These equations provide an efficient evaluation of the flow and heat transfer results $ReRa$ or $PrReRa$. Finally, we have complete correlations for flow and heat transfer characteristics of mixed convection in the presence of secondary flow, which are not possible to obtain by use of conventional scaling analysis.

With proper considerations, the CAPA technique could be extended to the thermal flow in rectangular channels of aspect ratio other than unity. However, it should be noted that the present version of CAPA still has some restrictions. It is not appropriate for the flows involving pure three-dimensionality, unsteadiness or turbulence at very high Re and/or very high Ra. To implement the CAPA technique for analysis of the above-mentioned complex flows is a challenge but worthwhile work.

References

[1] J. Palacios, Dimensional Analysis, Macmillan, New York, 1964.
[2] E. Buckingham, On physically similar systems: illustrations of the use of dimensional equations, Phys. Rev. 4 (1914) 345–376.
[3] E. Buckingham, Model experiments and the form of empirical equation, Trans. ASME 37 (1915) 263–296.
[4] H. Schlichting, Boundary Layer Theory, seventh ed., McGraw-Hill, New York, 1979.
[5] K.C. Cheng, S.W. Hong, G.J. Hwang, Buoyancy effects on laminar heat transfer in the thermal entrance region of horizontal rectangular channels with uniform wall heat flux for large Prandtl number, Int. J. Heat Mass Transfer 15 (1972) 1819–1836.
[6] A. Bejan, Heat Transfer, Wiley, New York, 1993.
[7] M.J.M. Krane, F.P. Incropera, A scaling analysis of the unidirectional solidification of a binary alloy, Int. J. Heat Mass Transfer 39 (1996) 3567–3579.
[8] C.Y. Soong, C.H. Chyuan, Investigation of buoyancy effects in non-isothermal rotating flows by scaling analysis and a novel similarity model, Chin. J. Mech. 14 (1998) 193–207.
[9] F.C. Chou, G.J. Hwang, Combined free and forced laminar convection in horizontal rectangular channels for high $ReRa$, Can. J. Chem. Eng. 62 (1984) 830–836.
[10] S.V. Patankar, Numerical Heat Transfer and Fluid Flow, McGraw-Hill, New York, 1980.

[11] G.J. Hwang, K.C. Cheng, Boundary vorticity method for convective heat transfer with secondary flow application to the combined free and forced laminar convection in horizontal tubes, in: Proceedings of the Fourth International Heat Transfer Conference, Versailles, Paris, vol. 4, Paper No. NC3.5, 1970.

[12] S.L. Lee, A strongly implicit solver for two-dimension elliptic differential equations, Numer. Heat Transfer B 16 (1989) 161–178.

[13] M.R. Spiegel, Mathematical Handbook of Formulas and Tables, McGraw-Hill, New York, 1968, pp. 32–33.